

## Research Article

## Constitutive Modeling of a Nb-Contained Advanced High-Strength Steel (AHSS) under Hot Compression Experiments

H. Chavilian, R. Vafaei and H. Sheikh\*

Department of Materials Engineering, Malek Ashtar University of Technology, Shahinshahr, Iran

## ARTICLE INFO

*Article history:*

Received 3 January 2022

Reviewed 20 January 2022

Revised 30 January 2022

Accepted 31 January 2022

*Keywords:*

Hot compression  
 Constitutive equation  
 High-strength steel  
 Dual phase steel

## ABSTRACT

In this study, the evaluation of hot forming behavior of an advanced high-strength steel (AHSS), namely Nb-Contained dual phase (DP) steel, is carried out using hot compression tests at temperatures of 850, 900, and 950°C with strain rates of 0.001, 0.01, and 0.1 (s<sup>-1</sup>). The resulting flow curves indicated the occurrence of dynamic recrystallization (DRX) at all different conditions of testing. Furthermore, based on the measured stress-strain data, material constants and activation energy (Q) were calculated for the peak stress. Additionally, the values of these constants were estimated for different true strains and the correlation between them and the strain has been illustrated by various diagrams. The comparison shows that the derived Arrhenius equation has an accepted accuracy for predicting the values of flow stress.

© Shiraz University, Shiraz, Iran, 2022

### 1. Introduction

Among advanced high-strength steels (AHSS), dual phase steels (DP) are very suitable candidates for automobile industries and complex structural components. This is mainly due to a very high tensile strength at ambient temperatures combined with good formability at relatively high temperatures along with high uniform elongation. Micro alloying additions to DP steels can further improve final mechanical properties of the products. Common micro alloying elements in these steels for automotive industries are mainly Ti and Nb. The presence of Nb in the chemical composition of the steel gives a finer grain size and consequently generates better energy absorption which in turn results in better car crash performance [1, 2].

Almost all hot forming of such steels is fairly complex and the evolution of microstructural characteristics depends on many parameters such as temperature, strain, and strain rate [3-5]. Therefore, occurrence of thermally activated phenomena such as dynamic recovery (DRV) and dynamic recrystallization (DRX) can have a profound influence on the flow behavior of such steels during hot deformation. Consequently, the choice of the best conditions of deformation is an important aspect of any industrial production [6-8]. Investigation of restoration processes and their kinetics during hot deformation can provide useful information for designing multi pass hot forming processes and can be evaluated by some various laboratory forming tests. In order to do so, it is necessary

\* Corresponding author

E-mail address: [sheikh\\_scientific@yahoo.com](mailto:sheikh_scientific@yahoo.com) (H. Sheikh)<https://doi.org/10.22099/IJMF.2022.42644.1208>

to investigate hot deformation behavior of the material using hot workability tests such as hot compression and hot torsion experiments. Mathematical expression of the flow behavior as constitutive equations can be employed for modeling the hot forming processes. There are various types of models such as Johnson-Cook, Arrhenius, and Zerilli-Armstrong that can predict the flow stress associated with acceptable accuracy [9]. Qin et al. [10] presented the true stress-strain curves of A602 CA nickel alloy by using a modified Arrhenius equation and achieved the desirable reliability. Also, Rakhshkhorshid et al. [11] and Yin et al. [12] used different approaches and obtained the acceptable constitutive equations to model the hot deformation behavior of AZ91 magnesium alloy and GCr15 steel, respectively.

Based on our knowledge, little work has been carried out on the evaluation of hot forming behavior of Nb-contained DP steels. In this investigation, deformation behavior of a selected dual phase steel is carried out by hot compression tests and the related constitutive equations are introduced.

## 2. Experimental Procedure

A Nb-contained dual phase steel was produced under conditions of laboratory melting with the composition of Table 1. The melting was carried out in a vacuum induction furnace and was further refined by the electroslag remelting (ESR) process. The homogenization treatment was carried out at 1100°C for 20 min followed by being cooled in air.

The standard cylindrical specimens for the hot compression tests were prepared by wire cut machine with the initial diameter of 10 mm and height of 15 mm. The single-hit hot compression tests were performed using a uniaxial test machine designed and built at the Malek Ashtar University of Technology. This device was designed to record the results of the compression of high-strength materials at high temperatures. The

machine was equipped with a computer-controlled resistance furnace under inert gas atmosphere and a precise data acquisition system. Before compression tests, the prepared samples were heated to temperatures ranging from 800 to 950°C and were kept for 5 min to achieve a uniform distribution of temperature. Then, the samples were isothermally pressed to 50% of their initial height at constant strain rates of 0.001-0.1s<sup>-1</sup>.

## 3. Results and Discussion

True stress-strain curves of the Nb-Contained DP steel during compression at various temperature and strain rates are shown in Fig. 1. The friction and adiabatic heating corrections were done on stress-strain curves using the approaches employed by Ebrahimi et al. [13] and Goetz et al. [14]. According to the shapes of corrected curves, it can be seen that all flow curves exhibit a single peak indicating the occurrence of DRX. However, at lower strain rates (0.001s<sup>-1</sup>) no significant peak can be observed and the difference between peak and plateau in flow curves decreases. This is mainly due to thermally activated softening mechanisms which occur at such strain rates because of their longer remaining time at the testing temperatures. In general, it is well understood that at lower strain rates and higher temperatures, the overall flow stress is lowered. As can be seen in Fig. 1, during first stage of deformation, stress increases sharply with strain due to work hardening until a peak value of stress is obtained. After the critical stress, the work softening starts to take effect. After the peak stress, the flow stress begins to descend to a steady state condition [15, 16]. The flow curves in Fig. 1 basically consist of three noticeable points: critical stress ( $\sigma_c$ ), peak stress ( $\sigma_p$ ), and steady state stress ( $\sigma_s$ ). Determination of  $\sigma_c$  is rather difficult because it cannot be determined directly from stress-strain curves. To this end, the stress rate hardening stress ( $\theta$ - $\sigma$ ) diagram was used to find the critical stress in this investigation, as shown in Fig. 2 [17]. Table 2 summarizes the data obtained from each flow curve of Fig. 1.

**Table 1.** Chemical composition of selected dual phase steel (wt.%)

%C	%Mn	%Cr	%Ni	%Nb	%Si	%Al	%P	%S	%Mo	%Fe
0.07	1.35	0.167	0.03	0.026	0.16	0.03	0.01	0.005	0.1	Bal.

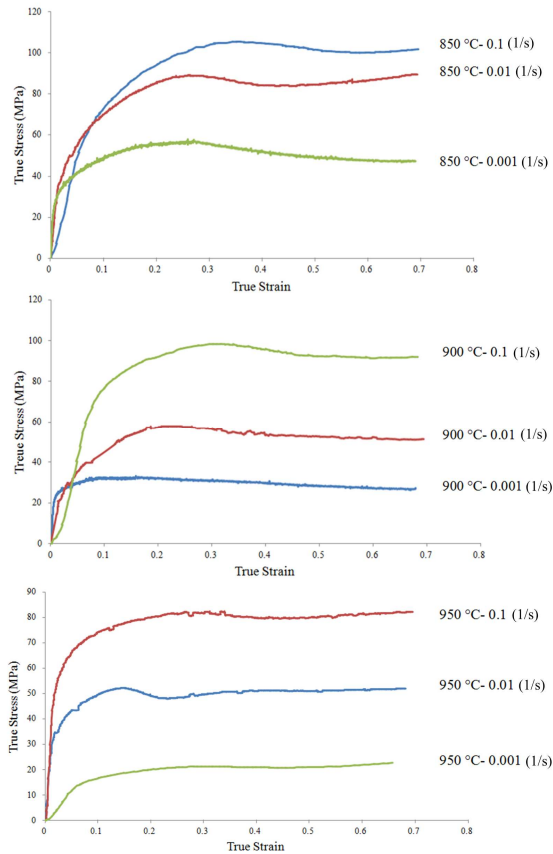


**Fig. 1.** Flow curves of Nb-Contained steel at different hot compression test conditions.

One of the common methods for determining the relationship between activation energy of hot deformation ( $Q$ ) and other parameters such as stress, temperature, and strain rate is studying the flow stress of material during hot compression test. Arrhenius type

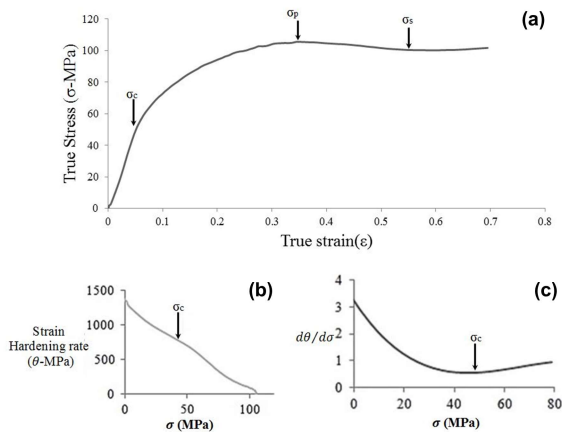


**Fig. 2.** Flow curve of Nb-contained steel during hot compression at 850°C and 0.1s<sup>-1</sup>: (a) strain-stress curve, (b) hardening rate vs stress, (c) first derivative of  $\theta$ .

**Table 2.** Values of peak and critical stress in different hot compression conditions for Nb-Contained steel

Strain rate (s <sup>-1</sup> )	Temperature (°C)	$\sigma_c$ (MPa)	$\epsilon_p$	$\sigma_p$ (MPa)
0.1	850	55	0.35	105
0.01	850	45	0.26	89
0.001	850	38	0.21	56
0.1	900	43	0.29	98
0.01	900	30	0.22	58
0.001	900	20	0.1	31
0.1	950	40	0.26	82
0.01	950	28	0.13	52
0.001	950	14	0.25	21

Eq. (1) expresses the relation between flow stresses, temperature, and strain rate [15, 16].

$$\dot{\epsilon} = AF(\sigma)\exp\left(\frac{-Q}{RT}\right) \quad (1)$$

where  $F(\sigma)$  is a function of flow stress expressed in the following three ways [15, 16]:

$$F(\sigma) = \sigma^n \quad \alpha\sigma < 0.8 \quad (2)$$

$$F(\sigma) = \exp(\beta\sigma) \quad \alpha\sigma > 1.2 \quad (3)$$

$$F(\sigma) = [\sinh(\alpha\sigma)]^{n'} \quad \text{for all } \sigma \quad (4)$$

where  $\dot{\epsilon}$  is the strain rate (s<sup>-1</sup>);  $R$  is the universal gas constant (8.31 J.mol<sup>-1</sup>K<sup>-1</sup>);  $T$  is the absolute temperature (K);  $Q$  is activation energy of hot deformation (kJ.mol<sup>-1</sup>) and  $\sigma$  is the true stress (MPa).  $A$ ,  $\beta$ ,  $\alpha$ ,  $n$ , and  $n'$  are the materials constants ( $\alpha = \beta/n$ ). The peak stress values ( $\sigma_p$ ) were used to plot the  $\ln\sigma$ ,  $\sigma$  and  $\ln\{\sinh(\alpha\sigma)\}$  versus  $\ln\dot{\epsilon}$  to estimate  $n$ ,  $\beta$ , and  $n'$ , respectively [18, 19]. Fig. 3, illustrates these diagrams for different conditions of compression. It can be seen that the resulting points have produced parallel lines. Since the slope of these lines is the same, the behavior of the material is assumed to be affected with similar mechanisms [18, 19]. In Table 3, the calculated constants are shown as mean values of inverted slope of the lines.

Mirzadeh [20] used a similar method to conduct a comprehensive study on the appropriateness of hyperbolic sine, power, and exponential descriptions of Zener–Hollomon parameter ( $Z$ ) in prediction of hot flow stress by consideration of the effect of strain on the material constants. He used innovative simplified methods and by comparing sine, power and exponential methods, despite

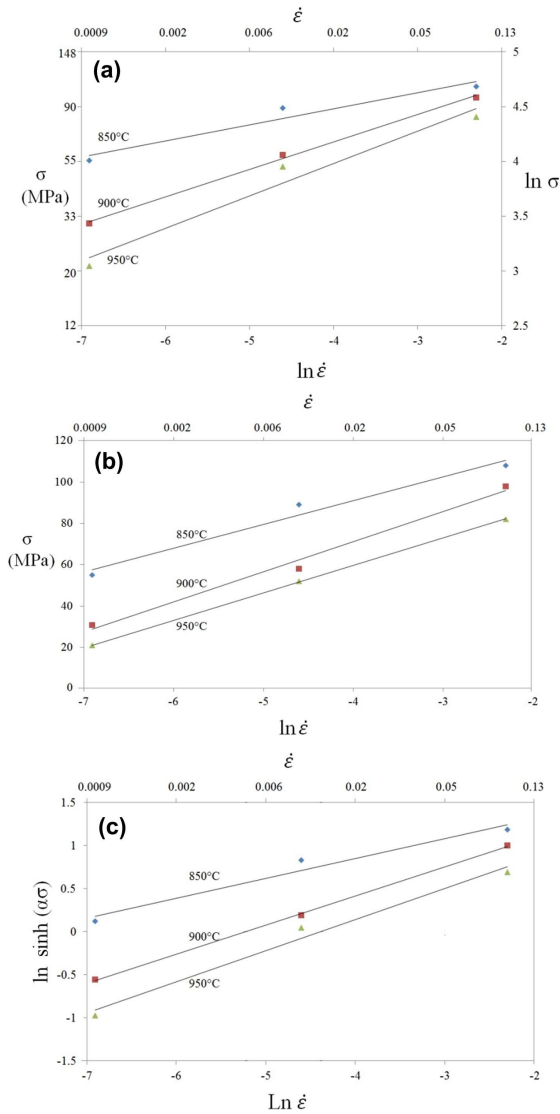


Fig. 3. Relations between: (a)  $\ln \sigma$  vs  $\ln \dot{\epsilon}$  to find  $n$ ; (b)  $\sigma$  vs  $\ln \dot{\epsilon}$  to find  $\beta$  and (c)  $\ln \sinh(\alpha\sigma)$  vs  $\ln \dot{\epsilon}$  to find  $n'$ .

Table 3. Constants values of Arrhenius equation calculated for the peak stress

$n$	$n'$	$\alpha$	$\beta$
4.33	3.22	0.018	0.076

finding some shortcomings and problems, he showed the efficiency of these methods to identify the hot deformation behavior of steels [20].

In order to determine the values of activation energy  $Q$ , it is necessary to first take a logarithmic value of Eqs. (2) to (4) and then differentiate the acquired equation for a constant strain rate. As a consequence, the following relations are achieved:

$$Q = R \cdot n \left[ \frac{\partial(\ln \sigma)}{\partial \left( \frac{1}{T} \right)} \right]_{\dot{\epsilon}} \quad (5)$$

$$Q = R \cdot \beta \left[ \frac{\partial(\sigma)}{\partial \left( \frac{1}{T} \right)} \right]_{\dot{\epsilon}} \quad (6)$$

$$Q = R \cdot n' \left[ \frac{\partial \ln \{ \sinh(\alpha\sigma) \}}{\partial \left( \frac{1}{T} \right)} \right]_{\dot{\epsilon}} \quad (7)$$

In a recent study by Saboori et al. [21], hot deformation activation energy was calculated in a similar way and the effectiveness of this method has been shown. As shown in Fig. 4, three diagrams of  $\ln \sinh(\alpha\sigma)$  vs  $1/T$ ,  $\ln \sigma$  vs  $1/T$  and  $\sigma$  vs  $1/T$  are plotted to estimate the average values of  $Q$  using Eqs. (5) to (7). Using the mean slope of the lines in Fig. 4 and the constants obtained from Table 3, the values of activation energy were calculated 293, 282, and 328  $\text{kJ} \cdot \text{mol}^{-1}$ , respectively. With regard to this point that the Eq. (7) is used for all values of stress, consequently the mean value of  $Q$  at  $\sigma_p$  can be assumed equal to 328  $\text{kJ} \cdot \text{mol}^{-1}$ .

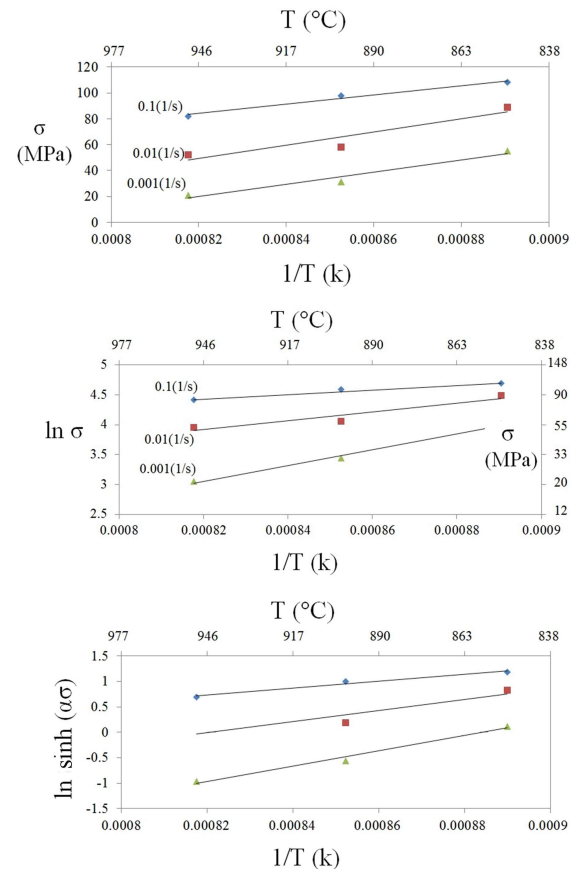


Fig. 4. Diagrams for determining the activation energy of Nb-Contained steel.

The constants of the Arrhenius equation can be varied at different strains and the reported values in Tables 3 only can be used to estimate  $\sigma_p$ . Therefore, a modified Arrhenius relation developed by Lin can be used to find strain dependent constants for all stress values [10, 22]:

$$\ln[\sinh(\alpha\sigma)] = \frac{\ln\dot{\epsilon}}{n} + \frac{Q}{nRT} - \frac{\ln(A)}{n} \quad (8)$$

According to the Eq. (5), all required constants of  $A$ ,  $n$ , and  $\alpha$  were calculated to determine the activation energy at interval values of 0.05 strain. As shown in Fig. 5, subsequently the calculated value of constants and activation energies were superimposed and the corresponding six order polynomial curves were extracted for  $n$ ,  $\alpha$ , and  $Q$  as following:

$$n = 4304.5\varepsilon^6 - 9732.6\varepsilon^5 + 8800.2\varepsilon^4 - 4089.4\varepsilon^3 + 1038.2\varepsilon^2 - 136.55\varepsilon + 11.93 \quad (9)$$

$$\alpha = 12.72\varepsilon^6 - 30.61\varepsilon^5 + 29.14\varepsilon^4 - 14.08\varepsilon^3 + 3.70\varepsilon^2 - 0.52\varepsilon + 0.05 \quad (10)$$

$$Q = 3 \times 10^8 \varepsilon^6 - 7 \times 10^8 \varepsilon^5 + 6 \times 10^8 \varepsilon^4 - 2 \times 10^8 \varepsilon^3 + 5 \times 10^7 \varepsilon^2 - 6 \times 10^6 \varepsilon + 69 \times 10^5 \quad (11)$$

Finally using the Eq. (9) to (11) and the estimated constants for different strains, the flow behavior of the steel was predicted by the following constitutive equation [10]:

$$\sigma = \frac{1}{\alpha} \ln \left\{ \left( \frac{Z}{A} \right)^{1/n} + \left[ \left( \frac{Z}{A} \right)^{2/n} + 1 \right]^{1/2} \right\} \quad (12)$$

where  $Z$  is the Zener–Hollomon parameter which is defined by the following relation [10]:

$$Z = \dot{\epsilon} \exp\left(\frac{Q}{RT}\right) \quad (13)$$

For example, as shown in Fig. 6, a comparison has been made between the experimental true stress-strain curve obtained for the temperature of 850°C and strain

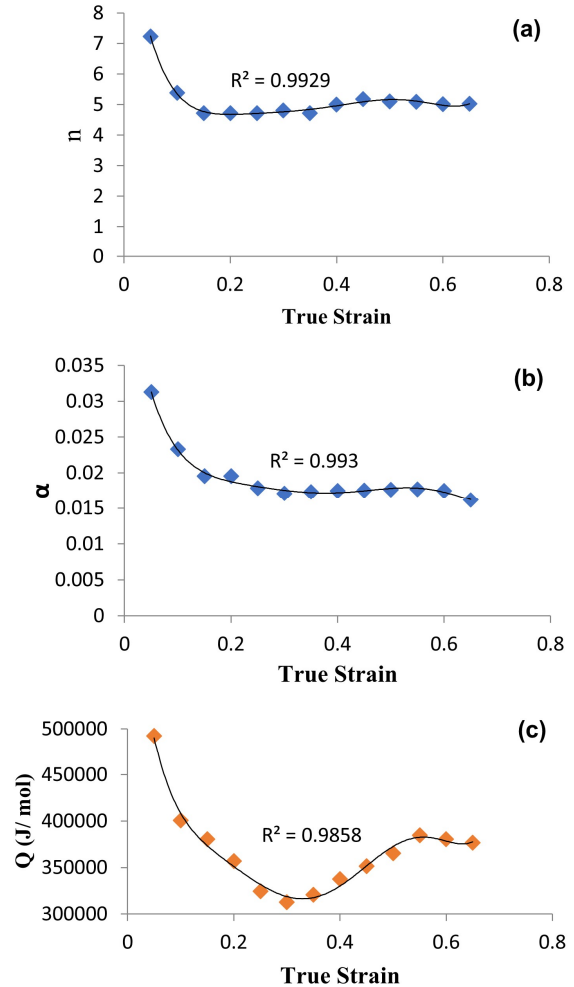


Fig. 5. Correlations between (a)  $n$ , (b)  $\alpha$ , (c)  $Q$  and true strain.

rate of  $0.1 \text{ s}^{-1}$  and the Eq. (9) to (11); as a result, it is clearly evident that a good agreement was observed illustrating the validation and accuracy of the proposed constitutive equation.

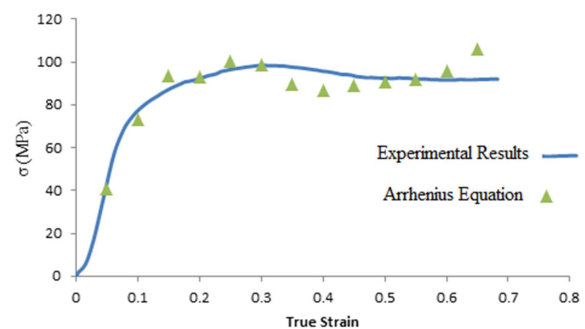


Fig. 6. Comparison between the experimental results and flow behavior predicted by a modified Arrhenius equation during compression at 850°C with the strain rate of  $0.1 \text{ s}^{-1}$ .

#### 4. Conclusion

Hot deformation behavior of a Nb-Contained steel was evaluated using hot compression test. At first, the values of peak and critical stresses for initiating dynamic recrystallization at various deformation conditions were calculated. Furthermore, it is calculated that at maximum applied stress, the value of activation energy for hot deformation is  $328 \text{ kJ.mol}^{-1}$ . It was found that there is an Arrhenius type relation between parameters such as flow stress, temperature, and strain rate to determine the flow behavior of such steel under hot compression. The estimation performed using the relation employing the strain dependent constants was found to be in good agreement with the experimental results showing the reliability of the employed constitutive equation.

#### Acknowledgments

The authors thank the Malek Ashtar University of Technology for the financial support of this study.

#### 5. References

- [1] N. Baluch, Z.M. Udin, C.S. Abdullah, Advanced high strength steel in Auto industries: an Overview, *Engineering, Technology & Applied Science Research*, 4(4) (2014) 686-689.
- [2] K. Mukherjee, S. Hazra, M. Militzer, Grain refinement in dual-phase steels, *Metallurgical and Materials Transactions A*, 40(9) (2009) 2145-2159.
- [3] W. Bleck, A. Frehn, J. Ohlert, Niobium in dual phase and trip steels, *International Symposium on Niobium, Proceedings. Niobium*, 2001, 727-752.
- [4] F.R. Xiao, Y.B. Cao, G.Y. Qiao, X.B. Zhang, L.I.A.O. Bo, Effect of Nb solute and NbC precipitates on dynamic or static recrystallization in Nb steels, *Journal of Iron and Steel Research, International*, 19(11) (2012) 52-56.
- [5] J.C. Cao, Q.Y. Liu, Q.L. Yong, X.J. Sun, Effect of niobium on isothermal transformation of austenite to ferrite in HSLA low-carbon steel, *Journal of Iron and Steel Research, International*, 14(3) (2007) 52-56.
- [6] H. Niakan, A. Najafzadeh, Effect of niobium and rolling parameters on the mechanical properties and microstructure of dual phase steels, *Materials Science and Engineering: A*, 527(21-22) (2010) 5410-5414.
- [7] J. Lee, S.J. Lee, B.C. De Cooman, Effect of micro-alloying elements on the stretch-flangeability of dual phase steel, *Materials Science and Engineering: A*, 536 (2012) 231-238.
- [8] A. Ghatei Kalashami, A. Kermanpur, A. Najafzadeh, Y. Mazaheri, Effect of Nb on microstructures and mechanical properties of an ultrafine-grained dual phase steel, *Journal of Materials Engineering and Performance*, 24(8) (2015) 3008-3017.
- [9] D. Samantaray, S. Mandal, A.K. Bhaduri, A comparative study on Johnson-Cook, modified Zerilli Armstrong and Arrhenius-type constitutive models to predict elevated temperature flow behaviour in modified 9Cr-1Mo steel, *Computational Materials Science*, 47(2) (2009) 568-576.
- [10] X. Qin, D. Huang, X. Yan, X. Zhang, M. Qi, S. Yue, Hot deformation behaviors and optimization of processing parameters for Alloy 602 CA, *Journal of Alloys and Compounds*, 770 (2019) 507-516.
- [11] M. Rakhshkhorshid, N. Mollayi, A.R. Maldar, A SVM model to predict the hot deformation flow curves of AZ91 magnesium alloy, *Iranian Journal of Materials Forming*, 4(2) (2017) 15-24.
- [12] F. Yin, L. Hua, H. Mao, X. Han, Constitutive modeling for flow behavior of GCr15 steel under hot compression experiments, *Materials & Design*, 43 (2013) 393-401.
- [13] R. Ebrahimi, A. Najafzadeh, A new method for evaluation of friction in bulk metal forming, *Journal of Materials Processing Technology*, 152(2) (2004) 136-143.
- [14] R.L. Goetz, S.L. Semiatin, The adiabatic correction factor for deformation heating during the uniaxial compression test, *Journal of Materials Engineering and Performance*, 10(6) (2001) 710-717.
- [15] E.I. Poliak, J.J. Jonas, Initiation of dynamic recrystallization in constant strain rate hot deformation, *ISIJ International*, 43(5) (2003) 684-691.
- [16] E.I. Poliak, and J. J. Jonas, A one-parameter approach to determining the critical conditions for the initiation of dynamic recrystallization, *Acta Materialia*, 44(1) (1996) 127-136.
- [17] A. Najafzadeh, J.J. Jonas, Predicting of the critical stress for initiation of dynamic recrystallization, *ISIJ International*, 46(11) (2006) 1679-1684.
- [18] H. Mirzadeh, A. Najafzadeh, Extrapolation of flow curves at hot working conditions, *Materials Science and Engineering: A*, 572(7-8) (2010) 1856-1860.
- [19] H.J. McQueen, N.D. Ryan, Constitutive analysis in hot working, *Materials Science and Engineering: A*, 322(1-2) (2002) 43-63.
- [20] H. Mirzadeh, A simplified approach for developing constitutive equations for modeling and prediction of hot deformation flow stress, *Metallurgical and Materials Transactions A*, 46(9) (2015) 4027-4037.

- [21] A. Saboori, A. Abdi, S.A. Fatemi, G. Marchese, S. Biamino, H. Mirzadeh, Hot deformation behavior and flow stress modeling of Ti-6Al-4V alloy produced via electron beam melting additive manufacturing technology in single  $\beta$ -phase field, *Journal of Materials Science & Engineering A*, 792 (2020) 139822.
- [22] Y.C. Lin, M.S. Chen, J. Zhong, Constitutive modeling for elevated temperature flow behavior of 42CrMo steel, *Computational Materials Science*, 42(3) (2008) 470-477.